HHS Public Access

Author manuscript

Mod Pathol. Author manuscript; available in PMC 2017 August 10.

Published in final edited form as:

Mod Pathol. 2017 May ; 30(5): 640–649. doi:10.1038/modpathol.2016.237.

Spitz nevi and Spitzoid melanomas - Exome sequencing and comparison to conventional melanocytic nevi and melanomas

Rossitza Lazova[1,2,3], **Natapol Pornputtapong**[2,3], **Ruth Halaban**[1], **Marcus Bosenberg**[1,2], **Yalai Bai**[2], **Hao Chai**[4], and **Michael Krauthammer**[2,5]

[1]Department of Dermatology, Yale University School of Medicine, New Haven, CT, 06520-8059

[2]Department of Pathology, Yale University School of Medicine, New Haven, CT, 06520-8059

[4]School of Public Health, Yale University School of Medicine, New Haven, CT, 06520-8059

[5]Program in Computational Biology and Bioinformatics, Yale University School of Medicine, New Haven, CT, 06520-8059

Abstract

We performed exome-sequencing of 77 melanocytic specimens composed of Spitz nevi (n=29), Spitzoid melanomas (n=27) and benign melanocytic nevi (n=21), and compared the results to published melanoma sequencing data. Our study highlights the prominent similarity between Spitzoid and conventional melanomas with similar copy number changes and high and equal numbers of ultraviolet-induced coding mutations affecting similar driver genes. Mutations in *MEN1, PRKAR1A*, and *DNMT3A* in Spitzoid melanomas may indicate involvement of the protein kinase-A pathway, or a role of DNA methylation in the disease. In addition to activating *HRAS* variants, there were few mutations in Spitz nevi, and few copy number changes other than 11p amplification and chromosome 9 deletions. Similarly, there were no large-scale copy number alterations and few somatic alterations other than activating *BRAF* or *NRAS* mutations in conventional nevi. A presumed melanoma driver mutation ($IDH1^{Arg132Cys}$) was revealed in one of the benign nevi. In conclusion, our exome data show significantly lower somatic mutation burden in both Spitz and conventional nevi compared to their malignant counterparts, and high genetic similarity between Spitzoid and conventional melanoma.

Introduction and Background

Recent exome sequencing studies have successfully uncovered several novel melanoma driver genes, including *PPP6C*, *RAC1* and *ARID2* (1–6), allowing for better understanding the pathways dysregulated in the disease. The results of the studies were also instrumental in classifying melanoma into four major subgroups, based on the mutational status of *BRAF*, *RAS* and *NF1* (3, 7, 8).

[3]These authors contributed equally

While much has been learned about the genetic causes of melanoma, the molecular changes underlying benign melanocytic lesions are known to a lesser degree. For example, small sequencing studies were performed on specific nevi subtypes, including congenital nevi (9). In addition, a recent study interrogated the mutational status of 182 cancer-related genes in 30 Spitz nevi (10), a type of benign nevus with characteristic 11p amplifications, concurrent *HRAS* mutations, and distinct histopathological features. However, we are not aware of a large-scale, comprehensive and unbiased genomic sequencing effort interrogating these lesions.

To address this, we exome-sequenced 29 Spitz nevi, 27 Spitzoid melanomas and 21 conventional melanocytic nevi in order to compare two types of melanocytic neoplasm: (1) Spitz nevi to Spitzoid melanomas, because they share common histopathological features such as epithelioid or spindled melanocytes, and (2) conventional melanocytic nevi to conventional melanoma (non-Spitzoid, referred to as melanoma below), using data from a recent exome-screen in melanoma (7). We hypothesized that a comprehensive exome-wide sequencing effort of these lesions should facilitate (a) a better understanding of the nevi mutational landscape, (b) insights into early mutational changes, and (c) a refined assessment of published melanoma driver genes by studying their presence or absence in nevi. Spitzoid lesions were of particular interest because there is an urgent need to discover markers that can accurately diagnose benign Spitz nevi present predominantly in children and young adults, and differentiate them from Spitzoid melanomas. The results of the studies can also address the question whether Spitz nevi and Spitzoid melanomas represent early and late stages of a distinct melanocytic subgroup with low UV exposure, as reported before (11).

Materials and Methods

Collection of samples and clinical data

The 29 Spitz nevi and 27 Spitzoid melanomas were retrieved from the Yale Spitzoid Neoplasm Repository. All cases were reviewed by six experienced dermatopathologists and only cases with an unequivocal consensus diagnosis were included in the study. Spitz nevi were defined as benign melanocytic nevi composed of large epithelioid, oval, or spindled melanocytes arranged in nests and/or fascicles (Figure 1a–c). Spitzoid melanoma was defined as a melanoma, histopathologically resembling a Spitz nevus and composed of large epithelioid melanocytes. Histopathological criteria used in the evaluation and classification of a lesion as a Spitzoid melanoma included (but were not limited to) the following: asymmetry, sheet-like growth pattern, expansile nodular growth, lack of maturation, ulceration of the epidermis, presence of mitotic figures, deep or atypical mitotic figures, deep extension into the subcutis, or large size (>1 cm) (Figure 1d–e). The following characteristics were recorded for Spitzoid melanomas: tumor thickness, primary anatomic location, age, gender, presence or absence of ulceration, and mitotic rate in accordance with the American Joint Committee on Cancer (AJCC). In addition, 21 conventional melanocytic nevi were also included. Clinical and histopathological data were recorded for all cases. Two 1-mm cores were obtained from each sample for DNA extraction. Adjacent normal tissue

was used as a control. Data for the conventional melanoma samples were reused from a prior study (7).

Exome sequencing, and variant calling

Exome sequencing and somatic variant calling was performed as described (3, 7). We used the NimbleGen SeqCap EZ Exome v2 capture kit, and performed paired-end sequencing on Illumina HiSeq. We used bwa and SAMtools for read alignment and single nucleotide variant calling, employing fully validated filtering criteria for identifying high quality DNA variants (3, 7). Tumor DNA sequencing was performed with a mean coverage of 231±56 impendent reads per base, mean error rate of 0.44%, and with 96% of the targeted bases covered with at least 20 independent reads. Normal DNA samples were sequenced with a mean coverage of 125±26 impendent reads per base, mean error rate of 0.36%, and with 93% of the targeted bases covered with at least 20 independent reads. Due to the slightly higher error rate compared to our earlier sequencing effort in conventional melanoma, we manually reviewed and filtered the top recurrent somatic hits in our samples.

Sanger validation

The mutations in *PRKAR1A* and *IDH1* were validated by Sanger sequencing of the DNA extracted from the formalin fixed and paraffin embedded tumors employing forward 5′-GAGTGCCAGCTTTACATGCC-3′ and reverse: 5′-CCGCATCTTCCTCCGTGTAG-3′ primers that amplified 211 bp in PRKAR1A, and 5′-GGCACGGTCTTCAGAGAAGCC-3′ and 5′-TGCCAACATGACTTACTTGATCCC-3′ primers that amplified 118 bp in IDH1, each surrounding the mutation site.

Copy number variant calling

Sequenza (12) was used to derive allele-specific copy number, ploidy and tumor purity from our data. We developed a script to extract arm-specific losses and gains from the Sequenza segmentation data. The normalized fold depth ratio was visualized using Circos (13).

Survival analysis

We assessed genetic changes for their effect on survival, using the univariate Cox proportional hazard model. Three common statistical tests were performed, namely likelihood ratio test, Wald test and score test. Common gene mutations and chromosomal aberrations were represented as Boolean values, i.e., true and false, and measured across the following known melanoma driver genes and mutations: *BRAF* (position 600), *NRAS* (positions 12,13,61), and any predicted damaging mutations in *NF1*, *TP53*, *CDKN2A*, *ARID2*, *PTEN*, *RAC1*, *CYP7B1*, and *PPP6C*. Chromosomal aberrations were recorded for each chromosome arm separately.

Machine learning and sample classification

Based on the similar features as discussed above, a decision-tree learning approach was used to classify nevi and melanomas based on exome sequencing data. An additional feature included the total number of somatic mutations, and chromosomal aberrations were assessed for common alternations found in melanoma, i.e., 6q, 8p, 9p and 10q losses, as well as, 1q,

6p, 7p, 7q, 8q, 17q and 20q gains. A decision tree classifier (14) in the Scikit-learn package performed the decision tree learning. The package allows the user to input tree complexity, that is number of decision node levels, and performs feature selection given a set of input features. The classifier was trained in two stages. In the first stage, we performed decision tree learning using a leave-one-out cross-validation. We then increased tree complexity by one for each run. This stage provided the optimal tree complexity for performing the classification, as well as the mean F1 score measured across the folds (we use the term accuracy for this measure across the remainder of the manuscript). In a second stage, we ran decision tree learning over the whole data set, setting the tree complexity to the one determined in the first stage. This stage produced a final tree with optimal features selected, and optimal cut-points for those features. We used all available patients for comparing Spitz nevi to Spitzoid melanomas. The algorithm in the Scikit-learn package performed weighted sampling to balance the number of samples in comparing conventional nevi to melanoma.

MC1R single nucleotide variant status

MC1R germline variants were classified as functional “R” or non-function “r” alleles based on published data (15–17) or, for novel variants, based on in silico predictions by PolyPhen and Sift. Unlike “r” alleles, R variants are thought to be damaging to protein function and/or known to be associated with red hair and light skin phenotypes. The members of each allele group are shown in Supplementary Table 2.

20/20 Analysis

We classified the top mutated genes based on the 20/20 heuristic rule (7, 18). The rule selects genes in which 20% or more of the observed somatic mutations are at recurrent sites, or in which 20% or more of the observed somatic mutations are inactivating (i.e., nonsense mutations, splice-site mutations, or InDels). Additionally, we used the Fisher’s exact test to compare the number of samples with somatic mutations in Spitzoid and conventional melanoma.

Results and Discussion

Sample cohort (see Supplementary Table 1)

The Spitz nevi cohort consisted of 29 patients, 15 females and 14 males (F:M= 1.1:1) that ranged in age between 1 to 35 years old (mean - 8.8; median –7). The lesions were distributed in decreasing order on the lower extremity (12), head and neck (7), upper extremity (7), and trunk (3). The follow-up ranged between 5 and 25 years with a mean of 14.6 years and a median of 14 years. All patients were alive and with no evidence of recurrence or metastasis at the conclusion of the study. The Spitzoid melanoma cohort consistent of patients 34 to 89 years old (mean - 64; median –65). There was no gender predominance. The lesions were distributed as follows in a decreasing order: trunk (8), lower extremity (6), upper extremity (6), and head and neck (5). Tumor thickness ranged between 1 mm and 9 mm with a mean of 3.7 mm and a median of 3.1 mm. The follow-up ranged between 0.5 and 15.5 years with a mean of 6.6 years and a median of 7 years. Seventeen patients were alive with no evidence of recurrence or metastasis, 6 were dead of disease, one expired of unknown cause, 2 patients were alive with disease, and one patient was lost to

follow-up at the conclusion of the study. The 21 conventional nevi came from patients between 3 months and 14 years of age (mean age=8.5 and median=11 years); 10 males and 11 females. In decreasing order, the location of the nevi was: head and neck (14), trunk (6), and lower extremity (1). The follow-up ranged between 3 and 12 years with a mean of 9.9 and median of 11 years. The 133 conventional melanoma samples, all from sun-exposed skin, have been described earlier (7). They consisted of 105 metastatic, and 28 primary samples. The majority of the latter were nodular melanomas (12), followed by superficial spreading melanoma (6), desmoplastic melanoma (1), spindle cell melanoma (1), lentigo maligna melanoma (1) and 7 melanomas of unknown type. Tumor thickness ranged between 0.2 mm and 22 mm with a mean of 3.9 mm and a median of 2.6 mm for the full cohort, and between 0.55 mm and 22 mm with a mean of 3.9 mm and a median of 3.3 mm for the primary samples only.

Mutational landscape

The number of somatic silent and non-silent single nucleotide variants, splice-site variants and InDels differed dramatically among the samples (Figure 2, Table 1, Supplementary Table 1). The number of mutations was significantly different between nevi and melanoma (both of the Spitzoid and conventional type), with 9±3 and 758±97 mutations in nevi and conventional melanomas (p = 2.35E-12), respectively, and 34±9 and 747±138 mutations in Spitz nevi and Spitzoid melanomas (p= 2.09E-05), respectively. On the other hand, there was no statistical difference in the mutational counts between the two types of nevi, and the two types of melanoma. All subtypes showed a characteristic UV mutation spectrum with ~90% C>T mutations in the dipyrimidine context (Figure 3).

There was a large overlap and commonalities in driver genes in Spitzoid melanomas and melanoma (7). Particularly, mutations affecting the MAPK pathway were present in 66% of the lesions, with 37% (10/27) *BRAF*-mutant, 18.5% (5/27) RAS-mutant and 11.1% (3/27) *NF1*-mutant Spitzoid melanomas. *NF1*-mutant Spitzoid melanomas harbored additional RASopathy gene mutations, as recently reported in conventional NF1-mutant melanomas (7). Of the three *NF1*-mutant Spitzoid melanomas, one sample harbored two *RASA2* (Pro530Leu, Gln500Ter), one a *PTPN11* (Thr73Ile), and another a *MAP2K1* (Pro124Leu) mutation (Supplementary Table 3). Spitzoid melanomas featured additional hotspot or inactivating mutations typically found in melanoma, including changes in *CDKN2A*, *TP53*, *RAC1*, *PTEN*, *IDH1* and *ARID2* (Supplementary Table 3). Our data, therefore, support the notion that conventional melanoma and Spitzoid melanoma are genetically similar, with undistinguishable somatic mutation counts, typical ultraviolet signature, and the same set of driver genes. These findings thus shed light on the ongoing controversy about whether these two lesions should be regarded as distinct entities (19, 20). The data also do not support a prior assessment that Spitzoid melanomas share a low-ultraviolet origin with Spitz nevi (11). We would like to note, that the current study did not assess the presence of kinase-fusion in Spitz nevi and Spitzoid melanomas (10). We repeated above analyses, comparing the sequenced Spitzoid melanomas, all primaries, to data from primary conventional melanoma only (Supplemantary Figure 1). As with the full cohort of conventional melanoma, we found no statistical difference in mutational counts, and large overlap in the known melanoma driver genes.

The majority (18/21) of conventional nevi harbored known oncogenes, with 47.6% (10/21) *BRAF* and 38% (8/21) *NRAS* mutations. In contrast, oncogenic *HRAS* p.Gly13/Gln61 mutations were present in only 17.2% (5/29) of Spitz nevi, as described (21, 22). A search for additional mutations across key melanoma drivers (7) revealed that one conventional nevus had the $IDH1^{Arg132Cys}$ mutant gene (Figure 4). Together, our data show that nevi, the conventional and Spitz type, harbor few ultraviolet mutations, and, with the exception of *BRAF*, *NRAS* and *HRAS*, lack additional changes in melanoma driver genes. Our finding that at least one nevus harbored $IDH1^{Arg132Cys}$ suggests a transition to a malignant state, as recently demonstrated in a large study showing progressive accumulation of mutations in the transition to malignant melanoma (23). Approximately 55% of Spitz nevi harbor kinase fusions (10), which was not assessed in the current study, and which likely account for the primary mutational event in the $HRAS^{WT}$ lesions.

Gene mutation burden

Our data allowed us to tabulate top mutated genes in our sequenced cohort. Given our small sample size, we used the 20/20 rule as organizing principle. The rule identifies presumed oncogenes and tumor suppressors by tabulating and thresholding, per gene, the ratio of recurrent and inactivating mutations, respectively. *BRAF*, *NRAS* and *HRAS* were the only recurrent oncogenic signature in conventional and Spitz nevi, and there was no gene that displayed a tumor suppressor signature (Supplementary Tables 4a and 4b). On the other hand, Spitzoid melanomas showed many of the same top mutated genes as conventional melanomas (Table 2 and 3), including a recurrent signature in *BRAF* and *IDH1* and inactivating signature in *ARID2* and *TP53*. Interestingly, the 20/20 rule identified *MEN1* and *PRKAR1A* as potential tumor suppressors in Spitzoid melanomas as both genes harbored mutations leading to early termination (Table 3, Figure 4). Germline inactivating mutations in *PRKAR1A* cause multiple neoplasia syndrome Carney Complex (24). The gene encodes the regulatory subunit type I-alpha of cAMP-dependent kinase, and loss-of-function increases protein kinase-A (PKA) activity leading to activated MAPK (25). Among other anomalies, Carney Complex patients feature intense skin pigmentation, pigmented epithelioid melanocytomas (26) and pituitary adenomas (27). Pituitary adenomas are also a hallmark of multiple endocrine neoplasia type 1 (MEN1) (27). These mutations occur rarely in conventional melanoma, suggesting involvement of the PKA pathway in the genesis of Spitzoid melanomas.

Copy number variant analysis

Conventional nevi did not show any region-wide copy number alterations (Figure 5). In Spitz nevi, we observed known 11p amplifications (22), in addition to hemizygous chromosome 9 deletions (Figure 5, Supplementary Figure 2), also described earlier (28). In contrast, Spitzoid melanomas mirrored typical copy number changes observed in melanoma, including 6q, 8p and 9p losses, as well as 6p and 8q gains (Figure 5).

Comparative genetic analysis

Using a statistical comparison of gene-level mutation burden, we identified higher mutation rate in *DNMT3A* in Spitzoid melanomas compared to melanomas (Supplementary Table 5) with three predicted damaging *DNMT3A* mutations in Spitzoid melanoma. Recurrent

DNMT3A mutations are associated with acute myeloid leukemia (29). Interestingly, an additional mutation was observed in Spitz nevi, supporting a possible role of DNA methylation in the pathogenesis of Spitzoid lesions.

We further used a machine learning approach to identify key differences among the sequenced lesions with regard the identified driver mutations, and/or chromosomal aberrations. The number of somatic coding single nucleotide variants (silent and non-silent) across the exome was selected as the major distinguishing feature between the benign and malignant conventional lesions. For our samples, this feature allows to distinguish between conventional melanoma and nevi with an accuracy of 93.5% (Supplementary Figure 3, right). Classification performance was 93.9% when comparing nevi with primary conventional melanoma only. For the comparison between Spitz nevus versus Spitzoid melanoma, an additional node counting the number of known melanoma driver mutations was essential to achieve a classification performance of 92.9% (Supplementary Figure 3, left). The below 100% accuracy is caused by some melanomas that do not exhibit key melanoma mutations or chromosomal aberrations. We also investigated whether data from small sequencing panels, rather than exome data, achieve similar classification performance. We thus simulated a targeted sequencing array covering 190 melanoma and other actionable cancer driver genes (30) by filtering our exome data for mutations in those genes only. We assumed that chromosome arm-level copy number assessment is still feasible using the smaller panel, for example by employing dedicated copy number variant sequencing probes (31). As seen in Supplementary Figure 4, due to the smaller capture region, the total number of observed somatic mutations is a less reliable decision criterion for distinguishing conventional nevi from conventional melanoma, and the algorithm selects the number of observed copy number events as an additional decision node, achieving a classification accuracy of 92.8% (Supplementary Figure 4, right). The decision tree for Spitzoid lesions is unchanged to the one discussed above, showing a classification accuracy of 91.1% for the simulated targeted array (Supplementary Figure 4, left).

Survival analysis

We analyzed whether any of the key mutational events in melanoma have an influence on patient survival. The tested mutations did not show a significant correlation with survival (Supplementary table 6), and while some copy number alterations were associated with survival, none achieved significance after multiple hypothesis correction.

MC1R analysis

Given the *PRKAR1A* findings that indicated possible involvement of the PKA pathway, we explored whether there were differences in *MC1R* variants among the skin lesions. Overall, there was no large difference among the subtypes, with 44.8%, 33.3%, 48.1% and 44.4% of Spitz nevi, conventional nevi, Spitzoid melanoma and conventional melanoma harboring the *MC1R* "R" variant (see Supplementary Table 2). *MC1R* Arg151Cys and Arg160Trp were present most frequently across the melanoma and nevi subtypes. There was a significant decrease in Arg151Cys frequency in Spitzoid melanoma compared to conventional melanoma (3.7% versus 22.6%, p=0.0238), and a significant increase for Arg160Trp (25.9% versus 11.2%, p=0.0438).

Limitation of the approach

While our sequencing approach follows good practices using a fully validated data analysis pipeline, we would like to note a couple of limitations. We noticed a slight increase in sequencing error rate (0.4% vs 0.2%) in the FFPE samples compared to our previously melanoma data, which were largely derived from fresh frozen tissue. Additionally, we collected two 1-mm cores from each sample for DNA extraction, with adjacent normal tissue used as a control. As a result, for a minority of collected normal tissue, we observed slight contamination with tumor cells, affecting somatic mutation calling. Also, we needed to exclude 4% (3/80) of the initially sequenced samples due to inadequate DNA quality. Finally, it should be noted that the discussed classification performance is valid for the samples included in this study, which does not contain ambiguous cases, such as atypical Spitz tumors.

Conclusion

We present exome-wide unbiased genomic sequencing data on Spitz nevi and conventional nevi, two benign lesions of the melanocytic lineage, and compare the findings to Spitzoid and conventional melanoma. Our data suggests that Spitzoid and conventional melanoma are genetically similar, with possibly involvement of the PKA and DNA methylation pathways in Spitzoid lesions. We also find a striking difference in the number of somatic single nucleotide variants, InDels and copy number changes between the benign and malignant lesions, a finding which may be exploitable as we move sequencing into clinical practice.

Supplementary Material

Refer to Web version on PubMed Central for supplementary material.

Acknowledgments

Research reported in this publication was supported by the Yale SPORE in Skin Cancer, funded by the National Cancer Institute, US National Institutes of Health, under award number 1 P50 CA121974 (M.K., N.P., R.H.) and Gilead Sciences, Inc. (R.L., Y.B.).

References

1. Gartner JJ, Davis S, Wei X, et al. Comparative exome sequencing of metastatic lesions provides insights into the mutational progression of melanoma. BMC genomics. 2012; 13:505. [PubMed: 23006843]
2. Hodis E, Watson IR, Kryukov GV, et al. A landscape of driver mutations in melanoma. Cell. 2012; 150:251–63. [PubMed: 22817889]
3. Krauthammer M, Kong Y, Ha BH, et al. Exome sequencing identifies recurrent somatic RAC1 mutations in melanoma. Nat Genet. 2012; 44:1006–14. [PubMed: 22842228]
4. Martin M, Masshofer L, Temming P, et al. Exome sequencing identifies recurrent somatic mutations in EIF1AX and SF3B1 in uveal melanoma with disomy 3. Nat Genet. 2013; 45:933–6. [PubMed: 23793026]
5. Stark MS, Woods SL, Gartside MG, et al. Frequent somatic mutations in MAP3K5 and MAP3K9 in metastatic melanoma identified by exome sequencing. Nat Genet. 2012; 44:165–9.
6. Wei X, Walia V, Lin JC, et al. Exome sequencing identifies GRIN2A as frequently mutated in melanoma. Nat Genet. 2011; 43:442–6. [PubMed: 21499247]

7. Krauthammer M, Kong Y, Bacchiocchi A, et al. Exome sequencing identifies recurrent mutations in NF1 and RASopathy genes in sun-exposed melanomas. Nat Genet. 2015; 47:996–1002. [PubMed: 26214590]
8. Genomic Classification of Cutaneous Melanoma. Cell. 2015; 161:1681–96. [PubMed: 26091043]
9. Charbel C, Fontaine RH, Malouf GG, et al. NRAS Mutation Is the Sole Recurrent Somatic Mutation in Large Congenital Melanocytic Nevi. J Invest Dermatol. 2014; 134:1067–74. [PubMed: 24129063]
10. Wiesner T, He J, Yelensky R, et al. Kinase fusions are frequent in Spitz tumours and spitzoid melanomas. Nat Commun. 2014; 5:3116. [PubMed: 24445538]
11. Bastian BC. The molecular pathology of melanoma: an integrated taxonomy of melanocytic neoplasia. Annu Rev Pathol. 2014; 9:239–71. [PubMed: 24460190]
12. Favero F, Joshi T, Marquard AM, et al. Sequenza: allele-specific copy number and mutation profiles from tumor sequencing data. Ann Oncol : official journal of the European Society for Medical Oncology / ESMO. 2015; 26:64–70.
13. Krzywinski M, Schein J, Birol I, et al. Circos: an information aesthetic for comparative genomics. Genome Res. 2009; 19:1639–45. [PubMed: 19541911]
14. Breiman L. Random Forests. Mach Learn. 2001; 45:5–32.
15. Beaumont KA, Shekar SN, Newton RA, et al. Receptor function, dominant negative activity and phenotype correlations for MC1R variant alleles. Hum Mol Genet. 2007; 16:2249–60. [PubMed: 17616515]
16. Raimondi S, Sera F, Gandini S, et al. MC1R variants, melanoma and red hair color phenotype: a meta-analysis. Int J Cancer. 2008; 122:2753–60. [PubMed: 18366057]
17. Pasquali E, Garcia-Borron JC, Fargnoli MC, et al. MC1R variants increased the risk of sporadic cutaneous melanoma in darker-pigmented Caucasians: a pooled-analysis from the M-SKIP project. Int J Cancer. 2015; 136:618–31. [PubMed: 24917043]
18. Vogelstein B, Papadopoulos N, Velculescu VE, et al. Cancer genome landscapes. Science. 2013; 339:1546–58. [PubMed: 23539594]
19. Mones JM, Ackerman AB. “Atypical” Spitz’s nevus, “malignant” Spitz’s nevus, and “metastasizing” Spitz’s nevus: a critique in historical perspective of three concepts flawed fatally. Am J Dermatopathol. 2004; 26:310–33. [PubMed: 15249862]
20. Cerroni L. Spitzoid tumors: a matter of perspective? Am J Dermatopathol. 2004; 26:1–3. [PubMed: 14726816]
21. Sarin KY, Sun BK, Bangs CD, et al. Activating HRAS mutation in agminated Spitz nevi arising in a nevus spilus. JAMA Dermatol. 2013; 149:1077–81. [PubMed: 23884457]
22. Bastian BC, LeBoit PE, Pinkel D. Mutations and copy number increase of HRAS in Spitz nevi with distinctive histopathological features. Am J Pathol. 2000; 157:967–72. [PubMed: 10980135]
23. Shain AH, Yeh I, Kovalyshyn I, et al. The Genetic Evolution of Melanoma from Precursor Lesions. N Engl J Med. 2015; 373:1926–36. [PubMed: 26559571]
24. Stergiopoulos SG, Stratakis CA. Human tumors associated with Carney complex and germline PRKAR1A mutations: a protein kinase A disease! FEBS Lett. 2003; 546:59–64. [PubMed: 12829237]
25. Robinson-White A, Hundley TR, Shiferaw M, et al. Protein kinase-A activity in PRKAR1A-mutant cells, and regulation of mitogen-activated protein kinases ERK1/2. Hum Mol Genet. 2003; 12:1475–84. [PubMed: 12812976]
26. Zembowicz A, Knoepp SM, Bei T, et al. Loss of expression of protein kinase a regulatory subunit 1alpha in pigmented epithelioid melanocytoma but not in melanoma or other melanocytic lesions. Am J Surg Pathol. 2007; 31:1764–75. [PubMed: 18059235]
27. Lecoq AL, Kamenicky P, Guiochon-Mantel A, Chanson P. Genetic mutations in sporadic pituitary adenomas--what to screen for? Nat Rev Endocrinol. 2015; 11:43–54. [PubMed: 25350067]
28. Gerami P, Scolyer RA, Xu X, et al. Risk assessment for atypical spitzoid melanocytic neoplasms using FISH to identify chromosomal copy number aberrations. Am J Surg Pathol. 2013; 37:676–84. [PubMed: 23388126]

29. Ley TJ, Ding L, Walter MJ, et al. DNMT3A mutations in acute myeloid leukemia. N Engl J Med. 2010; 363:2424–33. [PubMed: 21067377]

30. Hovelson DH, McDaniel AS, Cani AK, et al. Development and validation of a scalable next-generation sequencing system for assessing relevant somatic variants in solid tumors. Neoplasia. 2015; 17:385–99. [PubMed: 25925381]

31. Mason-Suares H, Kim W, Grimmett L, et al. Density matters: comparison of array platforms for detection of copy-number variation and copy-neutral abnormalities. Genet Med. 2013; 15:706–12. [PubMed: 23558256]

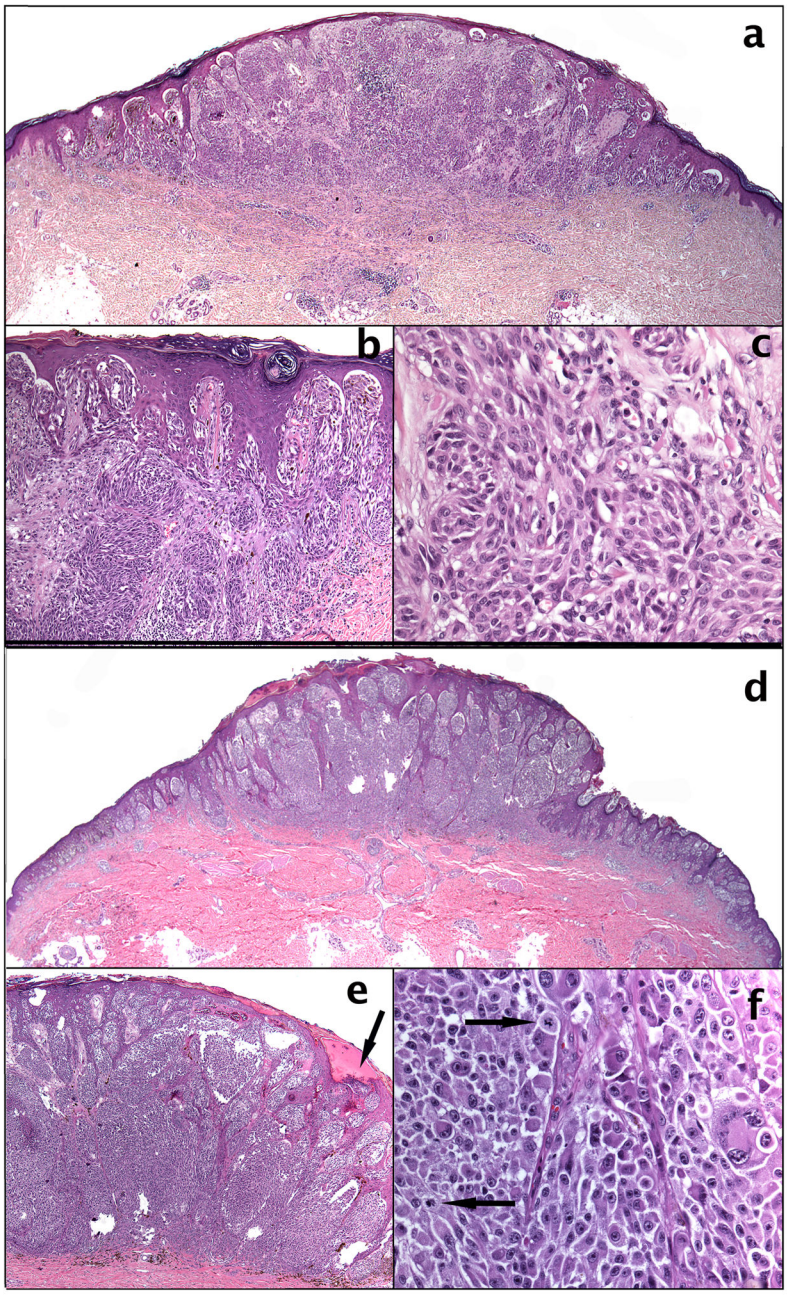

Figure 1.

a) A Spitz nevus (G728T) presenting as a symmetric, wedge-shaped and well-circumscribed melanocytic proliferation. b) Vertically oriented nests of melanocytes with clefts between them and the surrounding hyperplastic epidermis. c) The melanocytes are monomorphous and mitotic figures are absent. d) A Spitzoid melanoma (G762T) showing asymmetric growth pattern. e) The melanocytic nests vary markedly in size and shape and focally form sheets. The arrow marks a narrow ulceration of the epidermis. f) The melanocytes are pleomorphic and display prominent nucleoli. The two arrows point to mitotic figures in the dermis.

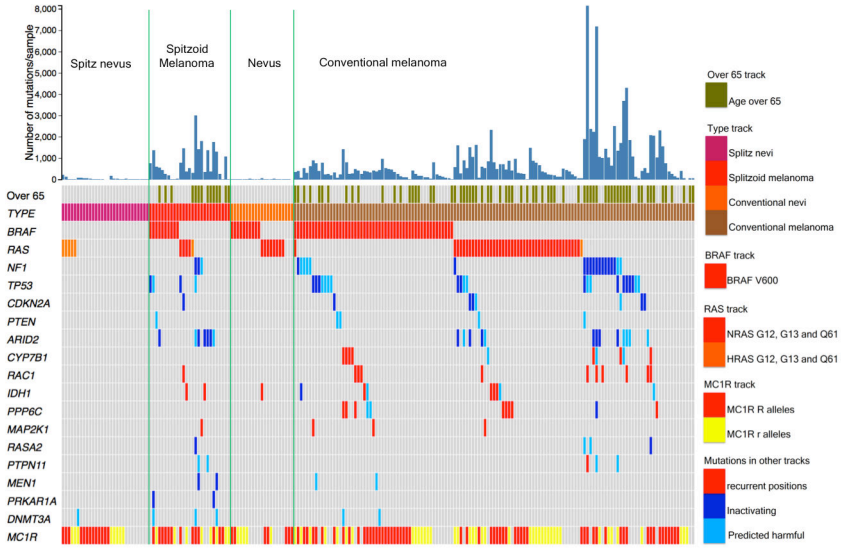

Figure 2.

Mutational landscape of Spitz nevi, Spitzoid melanomas compared to conventional nevi and melanomas. The 133 conventional melanomas correspond to paired samples from a previous publication (7).

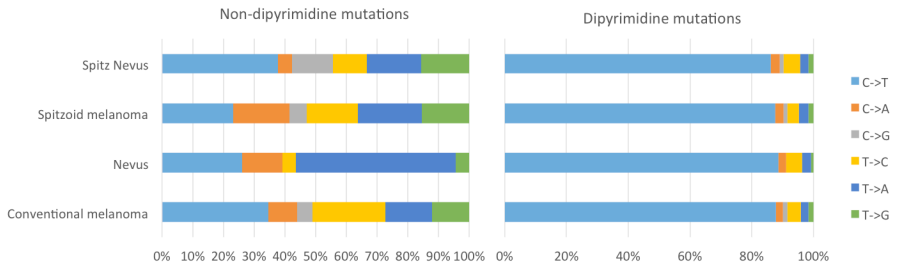

Figure 3.
Mutation spectrum. Observed mutations in non-dipyrimidines (left), and dipyrimidines (right).

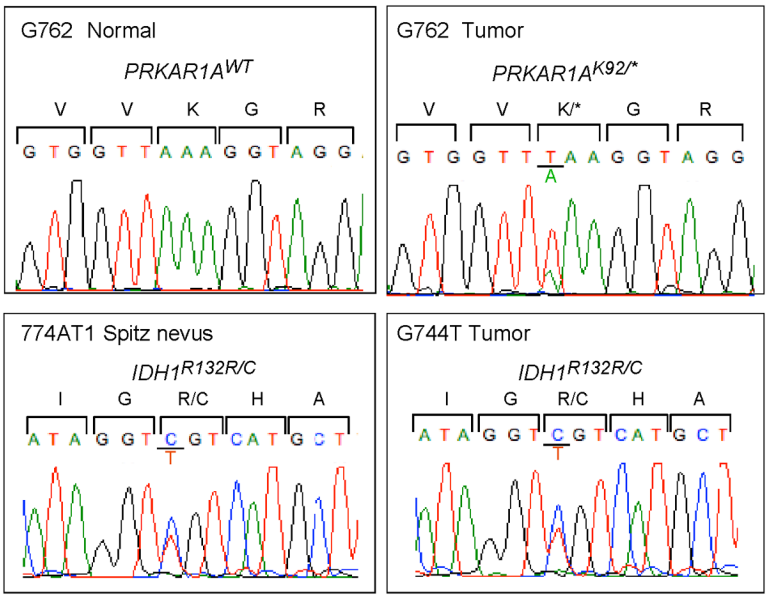

Figure 4.

Chromatogram of PRKAR1A^{K92*} in G762T Spitzoid melanoma (top); and IDH1^{R132C} in 774T1 Spitz nevus and G744 Spitzoid melanoma (bottom). The amino acid sequences adjacent to the mutation site is indicated

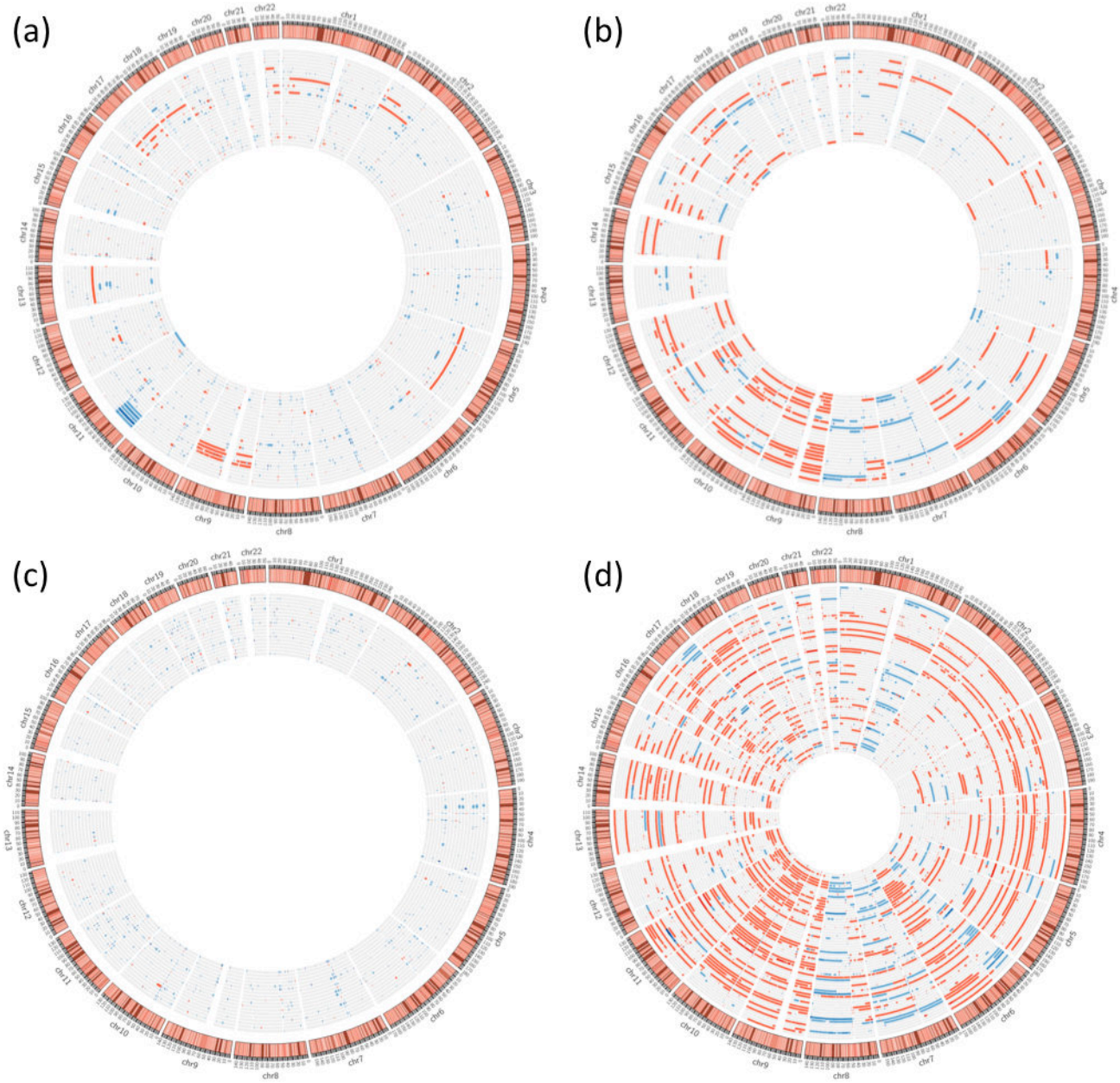

Figure 5.

Copy number alterations as shown by normalized log R ratio. These figures are plotted by Circos. (a) Spitz nevus; (b) Spitzoid melanoma; (c) conventional nevus and (d) conventional melanoma. Blue indicates copy number losses, and red indicates copy number gains.

Table 1

Exome-sequenced cohort. The 133 conventional melanoma samples correspond to paired samples from (7)

	Nevus	Spitz nevus	Spitzoid melanoma	Conventional melanoma
Number of samples	21	29	27	133
Sex				
Female	11	17	13	46
Male	10	12	14	87
Number of somatic mutations				
Mean with standard error	9.29±3.1	34.41±9.42	747.22±137.55	758.03±96.76
Age (year)				
Mean with standard error	8.25±0.63	8.76±1.3	64.11±2.77	67.24±1.18
Min	0.25	4	34	37
Max	14	25	89	94

Table 2

Somatic mutations at recurrent positions in Spitzoid melanomas. Filtered by % recurrent mutations, as defined by the 20/20 rule.

Gene	GeneID	% Recurrent Mutations	#Samples	Gene	GeneID	% Recurrent Mutations	#Samples
BRAF	ENSG00000157764	66.67	10	**MAP2**	ENSG00000078018	66.7	2
NRAS	ENSG00000213281	100	4	**RAB31**	ENSG00000168461	66.7	2
PCNXL2	ENSG00000135749	30.8	4	**ZSCAN2**	ENSG00000176371	66.7	2
STARD13	ENSG00000133121	42.9	3	**ABCC3**	ENSG00000108846	50	2
TBC1D9	ENSG00000109436	37.5	3	**LRRC1**	ENSG00000137269	50	2
BNIP2	ENSG00000140299	100	2	**LRRC16A**	ENSG00000079691	50	2
GORAB	ENSG00000120370	100	2	**NCOR1**	ENSG00000141027	50	2
IDH1	ENSG00000138413	100	2	**AXL**	ENSG00000167601	40	2
KLF7	ENSG00000118263	100	2	**DLG5**	ENSG00000151208	40	2
MMP2	ENSG00000087245	100	2	**ADAM23**	ENSG00000114948	33.3	2
MRPL1	ENSG00000169288	100	2	**GRIP1**	ENSG00000155974	33.3	2
NAA15	ENSG00000164134	100	2	**PCDHB2**	ENSG00000112852	33.3	2
SLC15A2	ENSG00000163406	100	2	**PLCL2**	ENSG00000154822	33.3	2
TMEM206	ENSG00000065600	100	2	**SAMD9**	ENSG00000205413	33.3	2
BCL10	ENSG00000142867	66.67	2	**SIK2**	ENSG00000170145	33.3	2
ERMP1	ENSG00000099219	66.7	2	**PHLDB2**	ENSG00000144824	22.22	2
FURIN	ENSG00000140564	66.7	2	**HEPH**	ENSG00000089472	20	2

Table 3

Somatic inactivating mutations (premature stop mutations, InDels and splice site variants) in Spitzoid melanomas. Filtered by % inactivating mutations, as defined by the 20/20 rule.

Gene	GeneID	% Inactivating Mutations	#Samples
ARID2	ENSG00000189079	66.7	6
HEPH	ENSG00000089472	30	3
AKAP9	ENSG00000127914	100	2
CEP128	ENSG00000100629	100	2
MEN1	ENSG00000133895	100	2
PRKAR1A	ENSG00000108946	100	2
SLC17A5	ENSG00000119899	100	2
STAT1	ENSG00000115415	100	2
TAOK1	ENSG00000160551	100	2
TOP2A	ENSG00000131747	100	2
ASCC3	ENSG00000112249	66.7	2
CCDC40	ENSG00000141519	66.7	2
CSPG4	ENSG00000173546	66.7	2
IPO7	ENSG00000205339	66.7	2
KIAA1328	ENSG00000150477	66.7	2
PML	ENSG00000140464	66.7	2
ATRNL1	ENSG00000107518	50	2
CEP192	ENSG00000101639	50	2
KMT2A	ENSG00000118058	50	2
TNRC6B	ENSG00000100354	50	2
AHNAK2	ENSG00000185567	28.6	2
NF1	ENSG00000196712	28.6	2
TP53	ENSG00000141510	28.6	2
TRIOBP	ENSG00000100106	28.6	2
COL4A1	ENSG00000187498	22.2	2
PLCG2	ENSG00000197943	22.2	2